


## Article

# Application of Deep Learning and WT-SST in Localization of Epileptogenic Zone Using Epileptic EEG Signals

Sani Saminu <sup>1,2,3,\*</sup> , Guizhi Xu <sup>1,2,\*</sup>, Zhang Shuai <sup>1,2</sup>, Isselmou Abd El Kader <sup>1,2</sup>, Adamu Halilu Jabire <sup>4</sup>, Yusuf Kola Ahmed <sup>3</sup>, Ibrahim Abdullahi Karaye <sup>1,2</sup> and Isah Salim Ahmad <sup>1,2</sup>

<sup>1</sup> State Key Laboratory of Reliability and Intelligence of Electrical Equipment, Hebei University of Technology, Tianjin 300130, China; zs@hebut.edu.cn (Z.S.); isselmou\_kaderi@yahoo.com (I.A.E.K.); karaye13264@yahoo.com (I.A.K.); isasalimahmad@gmail.com (I.S.A.)

<sup>2</sup> Key Laboratory of Electromagnetic Field and Electrical Apparatus Reliability of Hebei Province, Hebei University of Technology, Tianjin 300130, China

<sup>3</sup> Biomedical Engineering Department, University of Ilorin, Ilorin 240003, Nigeria; ahmed.yk@unilorin.edu.ng

<sup>4</sup> Electrical and Electronics Engineering Department, Taraba State University, Jalingo 660242, Nigeria; adamu.jabir@tsuniversity.edu.ng

\* Correspondence: saminu.s@unilorin.edu.ng (S.S.); gzxu@hebut.edu.cn (G.X.)

**Abstract:** Focal and non-focal Electroencephalogram (EEG) signals have proved to be effective techniques for identifying areas in the brain that are affected by epileptic seizures, known as the epileptogenic zones. The detection of the location of focal EEG signals and the time of seizure occurrence are vital information that help doctors treat focal epileptic seizures using a surgical method. This paper proposed a computer-aided detection (CAD) system for detecting and classifying focal and non-focal EEG signals as the manual process is time-consuming, prone to error, and tedious. The proposed technique employs time-frequency features, statistical, and nonlinear approaches to form a robust features extraction technique. Four detection and classification techniques for focal and non-focal EEG signals were proposed. (1). Combined hybrid features with Support Vector Machine (Hybrid-SVM) (2). Discrete Wavelet Transform with Deep Learning Network (DWT-DNN) (3). Combined hybrid features with DNN (Hybrid-DNN) as an optimized DNN model. Lastly, (4). A newly proposed technique using Wavelet Synchrosqueezing Transform-Deep Convolutional Neural Network (WTSST-DCNN). Prior to feeding the features to classifiers, statistical analyses, including t-tests, were deployed to obtain relevant and significant features at each approach. The proposed feature extraction technique and classification proved effective and suitable for smart Internet of Medical Things (IoMT) devices as performance parameters of accuracy, sensitivity, and specificity are higher than recently related works with a value of 99.7%, 99.5%, and 99.7% respectively.

**Keywords:** EEG; DNN; deep CNN; WT-SST; DWT; SVM



**Citation:** Saminu, S.; Xu, G.; Shuai, Z.; Kader, I.A.E.; Jabire, A.H.; Ahmed, Y.K.; Karaye, I.A.; Ahmad, I.S. Application of Deep Learning and WT-SST in Localization of Epileptogenic Zone Using Epileptic EEG Signals. *Appl. Sci.* **2022**, *12*, 4879. <https://doi.org/10.3390/app12104879>

**Academic Editors:**  
Francesco Donnarumma,  
Francesco Isgro and Roberto Prevete

Received: 8 April 2022

Accepted: 5 May 2022

Published: 11 May 2022

**Publisher's Note:** MDPI stays neutral with regard to jurisdictional claims in published maps and institutional affiliations.



**Copyright:** © 2022 by the authors. Licensee MDPI, Basel, Switzerland. This article is an open access article distributed under the terms and conditions of the Creative Commons Attribution (CC BY) license (<https://creativecommons.org/licenses/by/4.0/>).

## 1. Introduction

Epilepsy is one of the neurological disorders affecting many people at all levels of age. It may occur at any time, with an estimated population suffering from this disorder at more than 50 million, with most of the patients residing in developing countries [1]. An unprovoked seizure occurs due to a sudden change in the brain's cell electrical activity, which, if proper monitoring and diagnosing steps are not put in place, may lead to loss of consciousness, uncontrolled motions, jerking, and loss of memory [2,3]. These inconvenient and undesirable signs seriously undermine the quality of life of epilepsy patients as it is difficult for patients and doctors to predict when and where these seizures will occur. Therefore, it is of high importance to develop an efficient detection scheme and automate the system for monitoring epileptic seizures and assist clinicians in the proper and efficient diagnosis of this disease [4,5].

The development and integration of modern, smart, portable, and low-cost devices in our health care system known as the internet of medical things (IoMT) can monitor, track, and transmit data wirelessly with an online consultation in real-time scenarios is highly desirable [6–8]. An example of such a device was seen in the work presented by Lin et al. [9]. They proposed a real-time and low-power seizure detection system using a headband; they developed an application-based system that can record and transmit the data via a cloud. The efficiency of these devices largely depends on the accurate classification of these physiological signals, which, in turn, depend on the quality of feature extraction methods employed to extract the efficient and relevant signal information that characterize different signal properties [10,11]. This work proposed an efficient feature extraction technique suitable for smart IoMT devices due to its less computational complexity and optimized deep neural network detection pipeline.

This work uses focal and non-focal EEG signals, which depict the brain's electrical activity and can be studied by the neurologist to identify different parts of the brain, its function, and activities, including the epileptogenic part. Focal EEG signals are localized (i.e., indicating that a specific part of the brain is affected), while non-focal EEG signals are generalized (i.e., several parts are involved). However, manual and traditional interpretation of these signals, such as using the time-domain in extracting features, misses some useful information about the signal and renders this method ineffective [12].

In this paper, a comprehensive analysis of feature extraction and classification techniques for focal and non-focal EEG were studied using various signal analysis domains. An effective feature extraction algorithm was then developed using the time-frequency domain, statistical parameters, and nonlinear methods, as well as a new transform for extracting time-frequency sub-bands signals that have the ability to sharpen the time-frequency resolution and minimize the uneven distribution of energy in the wavelet transform domain. A new model was developed based on these features, while a two-dimensional-deep convolutional neural network (2D-DCNN) was adopted to distinguish the signal characteristics that are embedded in the EEG signals. The proposed method has the following novelties:

- Extraction of useful and relevant features using time-frequency domain and nonlinear approaches.
- Applying statistical parameters to reduce the feature's dimension for efficient classification
- Classification of focal and non-focal EEG signals using conventional techniques such as SVM and also deep learning approaches such as CNN with optimized function.
- Investigation of the most robust classifier by applying different SVM kernel functions and DNN architecture.
- Proposed a new technique based on the improved version of synchrosqueezing transform called wavelet transform synchrosqueezed transform (WT-SST) to extract tight time-frequency features and then classify with the proposed 2D deep CNN.

The rest of this paper is organized as follows. A review of relevant and related work is discussed in Section 2. Section 3 discusses the background concepts, and Section 4 presents the experimental system methodology of the proposed technique. Section 5 presents the results of the experiment, while Section 6 discusses the findings of the proposed models. Finally, Section 7 presents the conclusion, system improvement, and future direction.

## 2. Related Works

Many works have been reported in the literature on epileptic seizure detection and classification [11]. Several feature extraction techniques and various classifiers have been developed to achieve high efficiency and accuracy in the characterization of normal and abnormal spikes in epileptic seizure signals. Most of the existing studies on epilepsy detection and classification are focused on the classification of normal, ictal, and interictal EEG epileptic signal rhythms, as reported in [13,14]. However, only a few works reported the detection and classification of focal and non-focal EEG signals. These works include the proposed method developed in [15], where empirical wavelet transform has been employed for the classification of focal and non-focal EEG signals. Raghu and Sriraam [16] proposed a

detection and classification scheme using SVM for the detection of focal and non-focal EEG signals by employing neighborhood component analysis at the feature extraction stage. The resulting accuracy, sensitivity, and specificity of the scheme were 96.1%, 97.6%, and 94.4%, respectively. In Kumar and Rao [17], focal and non-focal EEG signals were detected and classified with various classifiers. A differential entropy was used for feature extraction while the accuracy, sensitivity, and specificity of 78.5%, 95.0%, and 95.0%, respectively, were recorded with a random forest classifier as the most robust among the experimented classifiers. Entropy measures were proposed and tested to differentiate between focal and non-focal EEG signals, as reported in Arunkumar et al. [18]. Focal and non-focal EEG signals were decomposed into sub-bands using Flexible Analytic Wavelet Transform (FAWT), while the features were then extracted using a fractal dimension in Dalal et al. [19]. Other works reported in the literature regarding the detection and classification of focal and non-focal EEG signals include one reported by Deivasigamani et al. [20], who developed a CAD system using complex wavelet transform with an ANFISS classifier. A non-parametric statistical approach was adopted in [21] as an unsupervised method. A Deep learning Convolutional Neural Network (CNN) was applied in [22,23]. Long short-term memory (LSTM) with a bi-directional learning system was used in the training phase, as reported in [24]. The average accuracy, sensitivity, and specificity reported in the LSTM system were 99.60%, 99.55%, and 99.65%, respectively. Several other approaches were proposed and reported in [25–30]. However, most of these works focused on either single domain feature extraction techniques, conventional classifiers, or artificial neural network classifiers. Therefore, this work proposed a comprehensive analysis by developing a model that combines several features from different domains. Furthermore, the proposed models include both conventional and recent deep learning structures. Another gap filled by this work is that most of the related works that used the same datasets as this work used a small number of datasets with 50 pairs of focal and non-focal EEG signals, but this work used a complete set of 3750 pairs of focal and non-focal EEG signals.

### 3. Materials and Methods

#### 3.1. Background

##### 3.1.1. Wavelet Transform-Synchrosqueezing Transform (WT-SST)

To overcome the problems associated with time-domain approaches in analyzing biomedical signals, Discrete wavelet transform (DWT) has been deployed by many researchers in analyzing physiological signals, including EEG. This is due to its ability to present a signal in the time-frequency domain suitable for analyzing non-stationary signals [31,32]. In this approach, focal and non-focal EEG signals  $x(n)$  are decomposed into sub-bands consisting of lower and higher frequency components using longer and shorter windows. These longer and shorter windows were achieved by using scaling and shifting functions on the signal. The scaling and shifting function corresponds to the low pass and high pass filters denoted as  $g[n]$  and  $h[n]$ , respectively [33,34]. These low pass and high pass filters produced the details and approximation coefficients, respectively. The process of filtering and decimation of EEG signals at each level continued until it reached the last level. Figure 1 demonstrates the three levels decomposition process. At each level, the decimation is achieved by downsampling the EEG signal into half to increase the frequency resolution of the signal.

Generally, wavelet functions is defined in Equation (1) as:

$$\Psi_{s,\tau} = \frac{1}{\sqrt{s}} \Psi\left(\frac{t-\tau}{s}\right) \quad (1)$$

where  $\Psi$  is the mother wavelet,  $s$  is called the scale parameter and  $\tau$  shift parameter.

From Equation (2), Wavelet transform is given as:

$$\gamma(s, \tau) = \int f(t) \Psi_{s,\tau}^*(t) dt \quad (2)$$

While Equation (3) defined Inverse wavelet transforms as:

$$f(t) = \iint \gamma(s, \tau) \Psi_{s, \tau}(t) d\tau ds \quad (3)$$

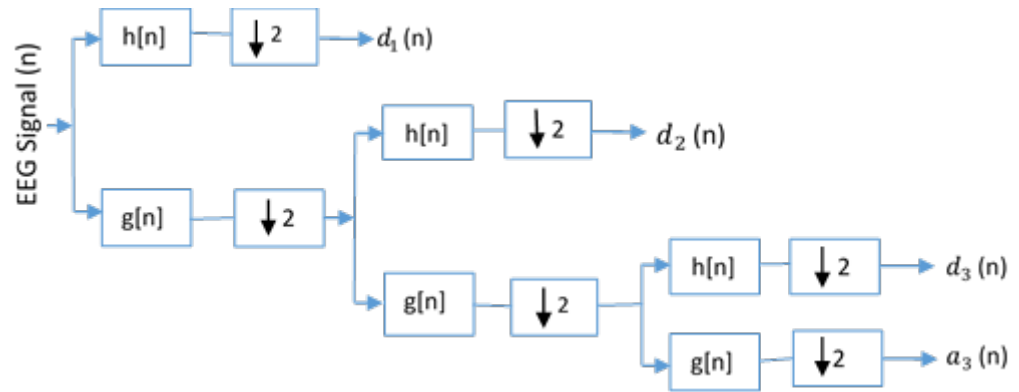


**Figure 1.** Decomposition of signals using DWT: Multiresolution analysis.

To improve and sharpen the resolution of time-frequency representations in wavelet transform, a recent special case of an improved version of the real-location approach was proposed by [35]. This approach reallocates the values in a time-frequency plane from a point  $\Re(\mathcal{g}, \mathcal{h})$  to a different point  $\Re(\mathcal{g}', \mathcal{h}')$  which is based on the local behavior of  $\Re(\mathcal{g}, \mathcal{h})$  around  $(\mathcal{g}, \mathcal{h})$ . The reallocation of coefficients results from a discrete-time continuous wavelet transform to obtain a compact time-frequency representation.

The continuous wavelet transform can be defined as in Equation (4):

$$\gamma_x^\Psi(\tau, s) = \frac{1}{s} \sum_{n=0}^{N-1} x(n) \Psi^* \left( \frac{n - \tau}{s} \right) \quad (4)$$

where  $\gamma_x^\Psi(\tau, s)$  is the element of scalogram matrix while  $\Psi^*$  represents the mother wavelet's complex conjugate. The instantaneous frequency estimation is used to sharpen our EEG signals time scale representations and its described as in Equation (5) [36,37].

$$\hat{\omega}(\tau, s) = \text{Re} \left[ \frac{1}{2\pi j} \frac{\gamma_x^\Psi(\tau+1, s)}{\gamma_x^\Psi(\tau, s)} \right] \quad (5)$$

$\text{Re}[\cdot]$  is the real part of EEG signals. Therefore, the WT-SST  $\omega^\lambda(\tau, s)$  can be described as in Equation (6):

$$\omega^\lambda(\tau, s) = \sum_{s=0}^S |\gamma_x^\Psi(\tau, s)| > \lambda \frac{1}{s} \gamma_x^\Psi(\tau, s) \delta[k - \hat{\omega}(\tau, s)] \quad (6)$$

where  $\lambda$  is the value of the threshold. In this work, we used a Morlet wavelet transform in the proposed WT-SST time-frequency.

### 3.1.2. Deep Neural Network

A deep neural network (DNN) is an extension of an artificial neural network consisting of dense hidden layers and many neurons. After every dense layer, dropout and batch normalization layers are included. It consists of many activation functions that can be implemented at different layers, such as a hyperbolic tangent and a rectified linear unit, among others. While the softmax activation function is implemented in this study's output layer, categorical cross-entropy is used as its loss function [38]. Two effective DNN structures were deployed and combined to form a robust hybrid DNN feature extraction and classification method. The two DNN structures are 1D-CNN and 2D-DCNN and are briefly explained as follows:

### 3.1.3. Convolutional Neural Network (CNN)

CNN is one of the most successful DNN structures applied in various research areas, such as image classification [39], speech analysis [40], and computer vision [41], among others, as compared to conventional neural networks. Recently, some researchers have investigated the efficacy of CNN in the detection and classification of epileptic seizures. This work aims to investigate the performance of CNN in the localization of the epileptogenic zone in the human brain.

The basic building block of CNN structures involves convolutional layers, pooling layers, and fully connected layers. With weighted parameters and the filters, the convolutional layer was designed. By convoluting the filters with input signals, the feature map vector was also developed [42]. For the input vector  $X$  and convolutional kernel  $K$ , the single output matrix  $Y$  can be expressed as in Equation (7):

$$Y_j = f\left(\sum_{i=1}^N X_i * K_{i,j} + B_j\right) \quad (7)$$

Each element is added with a bias element denoted as  $B_j$  while the nonlinear activation function is denoted as  $f$ .

This paper proposed a 1-dimensional CNN structure, as shown in Figure 2. It consists of 4-convolutional layers where the first layer accepts the input space and outputs the feature maps while the remaining convolutional layers accept and output the feature maps. The pooling layers accept the input from convolutional layers. The final feature vector is formed after transforming the features into a 1-dimensional array which is the input to a fully connected layer that computes the CNN output. This work employed the rectified linear unit (ReLU) as an activation function because it has a faster execution time when compared to the tanh and sigmoid activation functions.

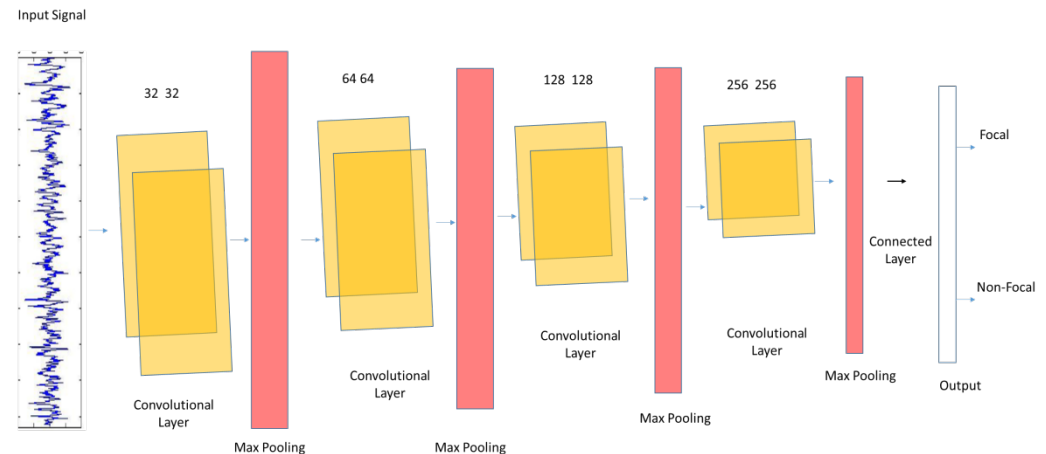


**Figure 2.** Architecture of 1D-CNN for classification of focal and non-focal using raw EEG signals, DWT features, and hybrid features.

### 3.1.4. 2D Deep CNN for WT-SST Features

To deal with time-frequency features obtained from WT-SST transform, we also proposed the 2-dimensional-deep CNN to effectively classified the focal and non-focal EEG signals due to its efficiency in the classification of physiological signals, such as medical images and in computer vision [43,44]. The structure of the proposed deep 2D-DCNN is that it consists of five layer-convolutional, max pooling, and fully connected layers. Figure 3 shows the number of feature maps in the layers, number of neurons, input and output signals, as well as convolution and max-pooling layers. As stated earlier, in this paper, we selected the number of samples as 2048 while the frequency points were 320. At each 2D

convolution layer denoted as the  $c$ th layer, the output of the feature map from that layer is  $Y_{i,j}^c$  and can be calculated as in Equation (8):

$$Y_{i,j}^c = f \left[ \sum_{a=0}^{m-1} \sum_{b=0}^{n-1} K_{ab}^c Y_{(i+a)(j+b)}^{c-1} + b_{ab}^c \right] \quad (8)$$

where  $m$  and  $n$  represent the size of the kernel, the activation function is  $f[\cdot]$  which is ReLU as in 1D-CNN;  $b_{ab}^c$  is the network bias. After obtaining the feature map from the convolution layer, the next is to compute the max pooling layer feature map as in Equation (9):

$$Y_{i,j}^c = \max \left[ Y_{(i+a)(j+b)}^{c-1} \right] \quad a \in (0, m), b \in (0, n) \quad (9)$$

The maximum value in the feature maps elements is represented as  $\max[\cdot]$  in a given range. The feature vector is obtained from the last max-pooling layer output while the output of the last fully connected layer has two neurons; it is computed as in Equation (9). At each fully connected layer, the feature vector for the  $c$ th layer is obtained by multiplying the weight matrix in the previous  $(c - 1)$ th layer. The output  $R(s)$  can be computed as in Equation (10):

$$R(s) = \frac{e^{w_s v}}{\sum_{s=1}^S e^{w_s v}} \quad (10)$$

where  $v$  is the  $(c - 1)$ th layer feature vector and the weight vector of the output layer connecting the  $S$ th neuron is denoted as  $w_s$ . During the network training, cross-entropy ( $C_e$ ) is used with the stochastic gradient descent (SGD) function. The  $C_e$  is given as:

$$C_e = -\frac{1}{U} \sum_{U=1}^U \sum_{S=1}^S Y_m(s) \log(R_m(s)) \quad (11)$$

where  $Y$  is denoted as output vector, while  $U$  is the minibatch size.  $\gamma$  is the parameter for the training the network at any instance, such as biases and kernels. To update the iteration parameters for  $(t + 1)$ th the rule is given as:

$$\gamma_{t+1} = \gamma_t + \frac{\beta}{U} \sum_{m=1}^U \nabla_{\gamma_t} [C_e(Y_m, R_m)] \quad (12)$$

where  $\nabla$  is the gradient operator,  $\beta$  is termed as the learning rate operator.

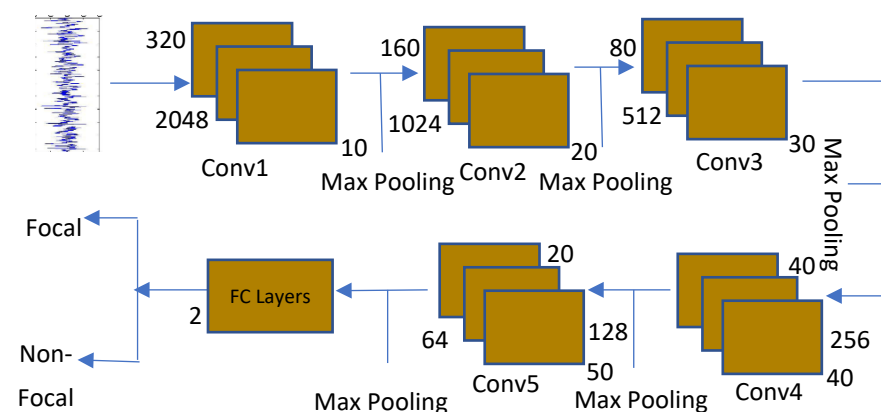


**Figure 3.** Architecture of 2D-DCNN for classification of focal and non-focal EEG using time-frequency WT-SST features.

### 3.1.5. Support Vector Machine

Our problem of identifying epileptogenic zone using focal and non-focal epileptic seizure signals is a binary classification, and as such, we employed an SVM classifier to classify our EEG signals. SVM is commonly used in biomedical signal analysis, especially with the problem of high dimensional feature vectors. It provides high accuracy and deals with a high



number of predictors. The SVM obtained and maximized the optimal hyperplane distance from high dimension feature space and that of each class's closest data sample. The SVM used regularization parameters to control the level of overlap between the kernel functions and each class [45,46]. An example of optimal hyperplane and the maximum margin for a two-dimensional separable problem with data points on the margin line representing support vectors are shown in Figure 4.

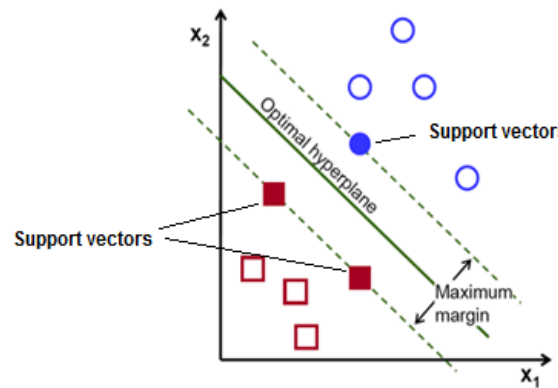


**Figure 4.** An example of a separable problem in a 2-dimensional space.

In this work, we optimized the SVM classifier by experimenting with different types of kernel functions such as linear, polynomials, and quadratic. The mathematical description of these kernel functions is expressed in Equations (13) and (14), respectively [47].

$$K(X, Y) = X^T Y \quad (13)$$

$$k(X_i, X_j) = (X_i, X_j)^d \quad (14)$$

where  $d$  is the number of polynomials and  $d(d \geq 1)$ . The function is called quadratic if  $d = 2$  or 3 [48].

#### 4. System Methodology

The proposed CAD system consist of the following stages:

- a. Data Acquisition
- b. Preprocessing
- c. Feature reduction and ranking
- d. Classification
- e. Performance analysis/evaluation

The block diagram of the proposed CAD system is shown in Figure 5.

##### 4.1. Data Acquisition

The dataset used in this study is publicly available and is known as the Bern-Barcelona database. It is recorded at the University of Bern, Department of Neurology, from five epilepsy patients that have longstanding pharmaco-resistant temporal lobe epilepsy. All the patients were screened for epilepsy surgery, and before the surgery, the recording of EEG signals was conducted as one of the diagnostic procedures. The EEG recording was conducted intracranially using depth electrode and intracranial strips with an AD-TECH (Racine, WI, USA) device in a multi-channel scenario. The number of channels is more or less than 64 channels using the standard international 10–20 system with Fz and Pz as reference electrode locations. Figure 6 shows the EEG signal acquisition arrangement with seizure hotspots marked in a red colour. Focal and non-focal EEG signals were carefully inspected by two certified neurologists visually; the first detected ictal signal from the EEG channels are referred to as focal signals, while the signals from the remaining channels are termed as non-focal EEG signals [24]. Of the focal and non-focal EEG signals, referred to as

x and y, 3750 pairs were acquired with a sampling frequency of 512 Hz and then filtered with a bandpass filter with a cut-off frequency of 0.5–150 Hz, with each signal consisting of 10,240 samples. One focal EEG channel was chosen at random from any patient, and another focal EEG channel from the neighboring selected channel was also selected and denoted as x and y, respectively. The details of this dataset can be found in [49]. In this work, complete sets of 3750 with both focal and non-focal signals were used in our analysis. Examples of focal and non-focal EEG signals are shown in Figure 7.

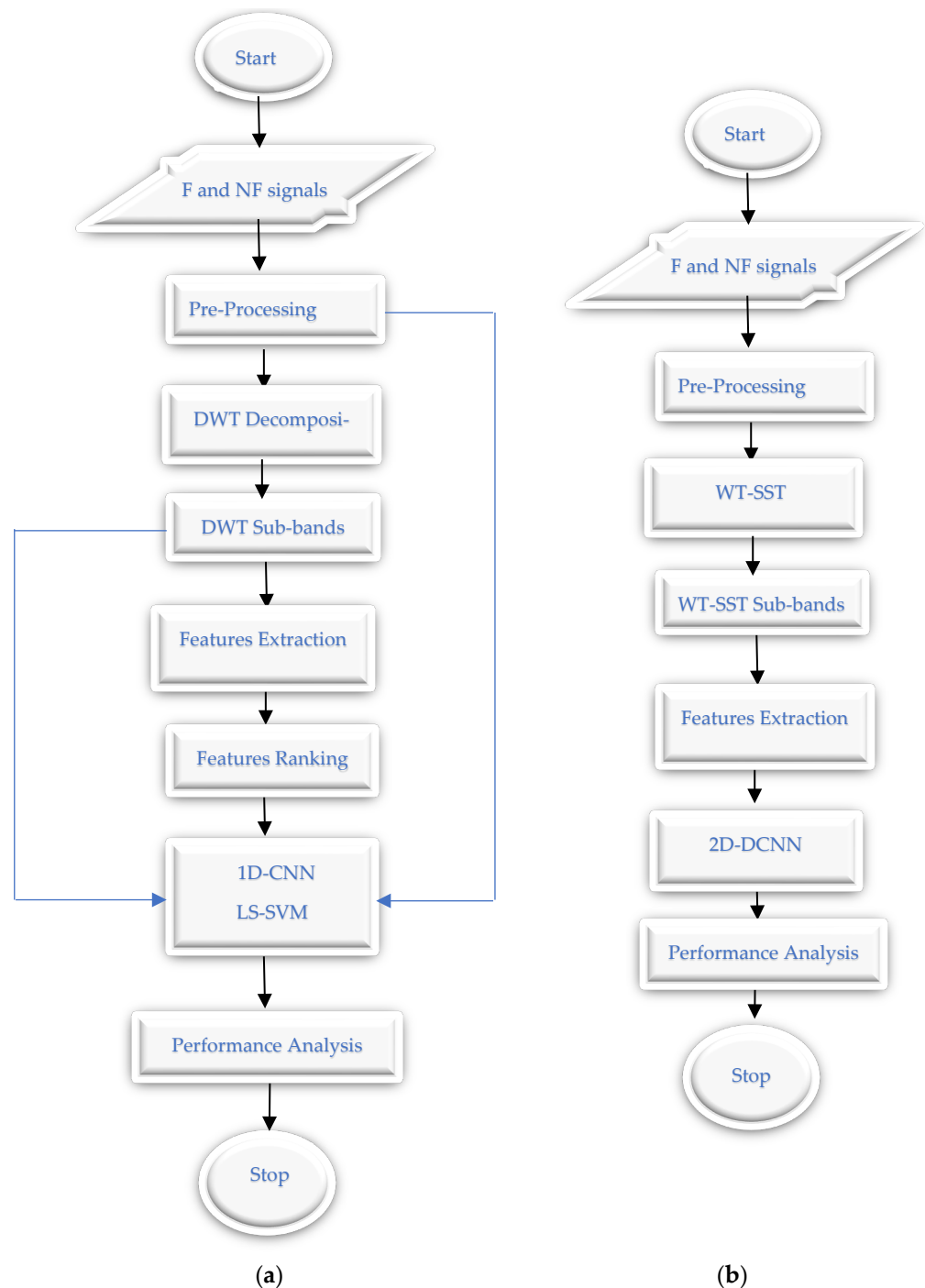


**Figure 5.** Block diagram of the proposed techniques, (a) classification of focal and non-focal EEG signals using DWT and hybrid features with SVM and 1D-CNN. (b) using WT-SST time-frequency matrix features with 2D-DCNN.



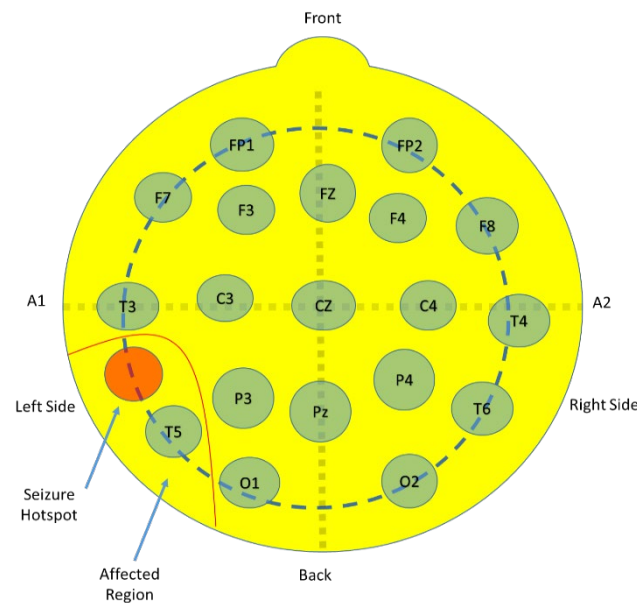


**Figure 6.** EEG signal acquisition set up using 10–20 international system with seizure hotspot shown in red colour [50].

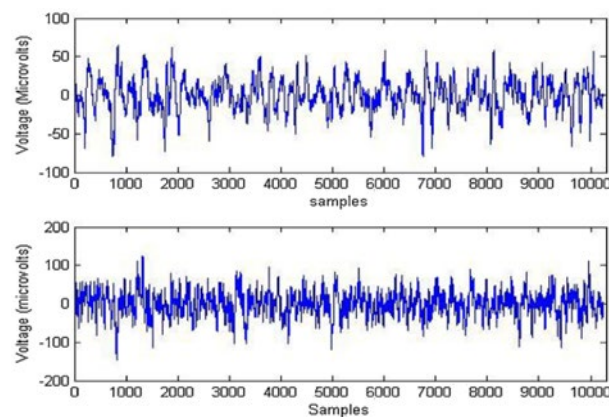


**Figure 7.** Example of Focal (**top**) and Non-Focal (**bottom**) EEG signals.

#### 4.2. Preprocessing, Feature Extraction and Feature Ranking

The preprocessing stage involves the removal of the artifacts and noise in the focal and non-focal EEG signals that are acquired during the recording of the signal. It also involves digital filtering, baseline correction, and signal re-referencing.

For the successful implementation of the CAD system for the detection and classification of focal and non-focal EEG signals, efficient and relevant features with low dimension but which still retain useful information are extracted. In this paper, wavelet transform has been deployed to extract time-frequency features. Afterwards, statistical parameters and nonlinear parameters were calculated to extract more meaningful features and reduce the feature dimension so that the classifier's computational complexity would be minimized. The computational complexity is one of the factors to be considered when developing smart IoMT devices. The raw EEG signals and wavelet features contain a lot of redundancy information that can render the classification process complex and difficult. Therefore, feature ranking and selection were carried out using a *t*-test in SPSS software to determine the probability (*p*) values. Parameters with a value higher than the critical value of 0.05 are considered non-statistically significant and can be dropped from the features. Figure 8 depicts the block diagram of feature vector formation from various domains and feature ranking.

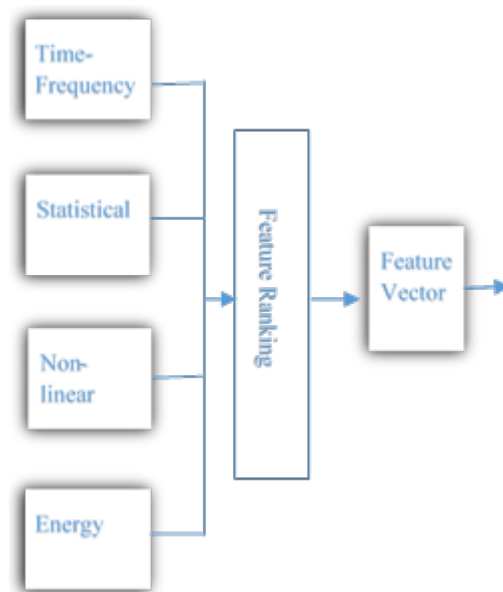


**Figure 8.** Feature extraction stage.

#### 4.2.1. Time-Frequency Features

Wavelet transform is used in decomposing the EEG signals into several sub-bands. Here, the Daubechies mother wavelet is selected because it was proven in the literature to be suitable for decomposing EEG signals [51]. The level of decomposition is selected as 10 to capture all the signal coefficients.

#### 4.2.2. Statistical Features

The statistical parameters such as mean, median, and standard deviation, among others, as summarized in Table 1, have been computed at each sub-band of the EEG signal. The details and approximate coefficient at  $d_1 - d_{10}$  and  $a_{10}$  were extracted, respectively, decreasing the signal dimension for an appropriate input to the classifier.

**Table 1.** Summary of Statistical Parameters deployed in this study.

Title 1	Name	Theory
Statistical Domain	Mean	$\mu = \frac{1}{M} \sum_{j=1}^M  y_j $
	Median	$M = \left(\frac{n+1}{2}\right)^{th} \text{ term}$
	Mode	$M = \left(\frac{n+1}{2}\right)^{th} \text{ term}$
	Maximum Minimum	$Max = \max(f_i)$ $Min = \min(f_i)$
	Standard Deviation	$\sigma = \sqrt{\frac{1}{M} \sum_{j=1}^M (y_j - \mu)^2}$
	Skewness	$\phi = \sqrt{\frac{1}{M} \sum_{j=1}^M \frac{(y_j - \mu)^3}{\sigma^3}}$
	Kurtosis	$\phi = \sqrt{\frac{1}{M} \sum_{j=1}^M \frac{(y_j - \mu)^4}{\sigma^4}}$

#### 4.2.3. Nonlinear Features

To increase the robustness of features extracted for this classification, nonlinear features were extracted using linear analysis, such as sample entropy, fuzzy entropy, and approximate entropy, as summarized in Table 2.

**Table 2.** Summary of Nonlinear Entropies Parameters Computed in this study.

Title 1	Name	Theory
Entropy Features	Shannon	$En_{shan} = \sum_{n=1}^x S_n \log_2 S_n$
	Renyi	$En_{renyi} = \frac{1}{1-\alpha} \sum_{n=1}^x \log(S_n)^\alpha$
	Log Energy	$En_{logen} = \sum_{n=1}^x \log(s_n^2)$
	Permutation	$En_{per} = -\sum_{n=1}^{x!} S_n \log_2 S_n$

#### 4.3. K-Fold Cross Validation

To increase the performance and evaluate the validity of the machine learning classifiers, a cross-validation approach is usually employed to divide the dataset into  $k$  number of sub-sets, known as  $k$ -fold cross-validation. In this approach, the features are divided into  $k$ -fold group sub-sets with a single set selected as the test data while the remaining subsets are selected as the training data. For example, this work employed 10-fold cross-validation, the dataset is divided into 10 subsets, and at each subset, the data are sub-divided into one for test data and the remaining nine for training data, so the alteration would be carried out ten times. An example of 10-fold cross-validation is described in Figure 9.

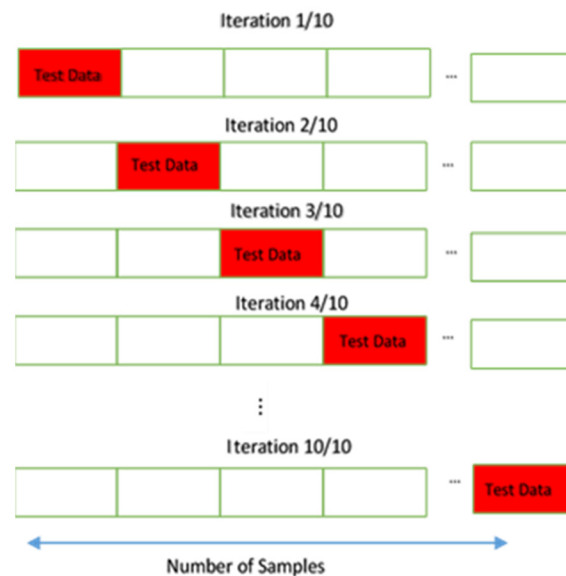


**Figure 9.** Description of 10-fold cross-validation.

## 5. Results

This paper carried out an extensive and comprehensive analysis of various feature extraction, detection, and classification techniques to classify focal and non-focal EEG signals that help doctors in the localization of the epileptogenic zone for surgical operations. Moreover, the paper proposed an efficient and robust feature extraction scheme based on statistical, time-frequency and nonlinear features. The adopted hybrid techniques consist of various features combined with different SVM approaches and several deep neural network structures. Focal and non-focal EEG datasets were acquired and downloaded from the Bern-Barcelona database. Each focal and non-focal EEG signal consists of a pair of signals corresponding to two channels denoted as  $x$  and  $y$ . In this work, we adopted the approach employed in [52] of computing the average value of features calculated from the

EEG rhythm. For this, 7500 EEG records were randomly selected for each signal to form the complete EEG records for training and testing as a .txt file. The dataset was divided into training and test sets with 70% and 30% standards for training and validation, respectively, in the SVM classifier models. While, for the DNN models, the dataset was divided into 80% and 20% for training and testing, respectively. Out of the 80% assigned for training, the standard 70% and 30% were used for training and validation. For preprocessing and feature extraction, a MATLAB environment was utilized for those operations, while an efficient DNN library that runs on top of TensorFlow, known as Keras, was employed during the DNN modelling process. For each training cycle, 100 was chosen as the batch size. A 10-fold cross-validation was used in training and test instances.

Features from different domains have been tested using a *t*-test in SPSS software to obtain significant features. After performing the test, 78 features were deployed as hybrid features because their *p*-value was less than 0.05, which means that they are statistically significant. Some features, such as dimensional fractal features, were discarded in the analysis because their *p*-value was higher than 0.05. For the WT-SST time-frequency domain, 16 features in the FC4 layer were found to be statistically significant as their *p*-value was less than 0.05. The proposed 1D-CNN was used to classify the raw EEG signals and DWT features, while the time-frequency matrix of focal and non-focal EEG signals resulting from WT-SST was used in the classification with 2D-DCNN architecture, which extracts learnable feature maps.

The classifier's performance is evaluated using the following performance parameters:

$$\begin{aligned}\text{Sensitivity} &= \frac{TP}{TP + FN} \\ \text{Specificity} &= \frac{TN}{TN + FP} \\ \text{Accuracy} &= \frac{TP + TN}{TP + FP + FN + TN} \\ \text{Precision} &= \frac{TP}{TP + FP} \\ \text{F1\_Score} &= 2 \frac{\text{Precision} * \text{Sensitivity}}{\text{Precision} + \text{Sensitivity}}\end{aligned}$$

where TP is True Positive (correctly identified), FP is False Positive (incorrectly identified), FN is False Negative (incorrectly rejected), TN is True Negative (correctly rejected).

### 5.1. Performance Analysis of Discrete Wavelet Features

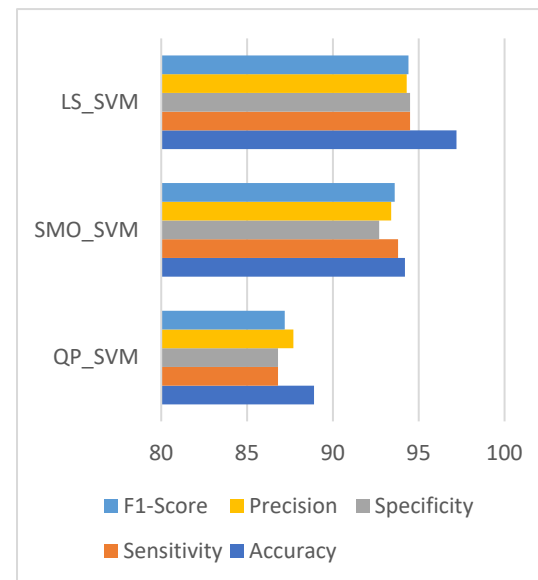
The performance of discrete wavelet features was evaluated with SVM and the 1D-CNN deep neural network with gradient descent. Different kernel functions and various types of SVM were experimented with, as depicted in Table 3 and Figure 10, respectively. From the table and Figure, it was clearly shown that LS\_SVM with polynomial kernel function performs better than other kernel functions and SVM types with an accuracy, sensitivity, and specificity of 97.2%, 94.5%, and 94.5%, respectively. Table 4 shows the comparison of the performance of the deep learning network with the best SVM classifier, where the former outperforms the latter with 98.8%, 97.3%, and 97.7% for accuracy, sensitivity, and specificity, respectively.

**Table 3.** Different kernel function of SVM with DWT features.

Kernel Function	Sen(%)	Spe(%)	Acc(%)	Prec(%)	F1-Sc(%)
Linear	87.3	87.3	86.1	86.6	86.9
Quadratic	92.6	92.6	93.0	92.4	92.5
Polynomial	94.5	94.5	97.2	94.3	94.4
rbf	85.3	84.2	82.5	83.2	84.2

**Table 4.** Comparison between 1D-CNN and SVM for DWT features.

Classifier	Sen(%)	Spe(%)	Acc(%)	Prec(%)	F1-Sc(%)
DWT-DNN	97.3	97.7	98.8	98.8	98.0
DWT-SVM	94.5	94.5	97.2	94.3	94.4

**Figure 10.** Performance of Different SVM types for Time-Frequency features.

### 5.2. Performance of Hybrid Features and WTSST-DCNN

The DWT features were combined with statistical and nonlinear features, and the performance of this proposed approach was experimented with and evaluated with the deep neural network and SVM classifier. Different kernel functions of SVM and three types of SVM were experimented with to find the optimum and most robust classifier. Figure 11 shows the proposed approach's performance for different types of SVM, while Table 5 shows different SVM kernel function performances. Finally, a comparison of 1D-CNN, best SVM classifier performance, and the performance of the proposed new transform WTSST-DCNN were evaluated, as presented in Table 6. From the table and figure, it is clearly shown that the polynomial kernel function with the LS\_SVM method outperforms other kernel functions and SVMs with accuracy, sensitivity, and specificity of 99.3%, 99.5%, and 99.0, respectively. However, the proposed deep learning network of WTSST-2D-DCNN shows an improvement in performance when compared to the SVM best-optimized classifier with 99.7%, 99.5%, and 99.7% accuracy, sensitivity, and specificity, respectively.

**Table 5.** Different kernel function of SVM for hybrid features.

Kernel Function	Sen(%)	Spe(%)	Acc(%)	Prec(%)	F1-Sc(%)
Linear	97.5	95.5	97.5	96.8	97.1
Quadratic	99.4	98.9	99.0	99.2	99.3
Polynomial	99.5	99.0	99.3	99.3	99.4
rbf	88.8	88.1	87.6	88.7	88.7

**Table 6.** Comparison between DNN and SVM for hybrid features and WTSST-DCNN.

Classifier	Sen(%)	Spe(%)	Acc(%)	Prec(%)	F1-Sc(%)
Hybrid-1D-CNN	99.4	99.3	99.4	99.3	99.3
Hybrid-SVM	99.5	99.0	99.3	99.3	99.4
WTSST-DCNN	99.5	99.7	99.7	99.7	99.6

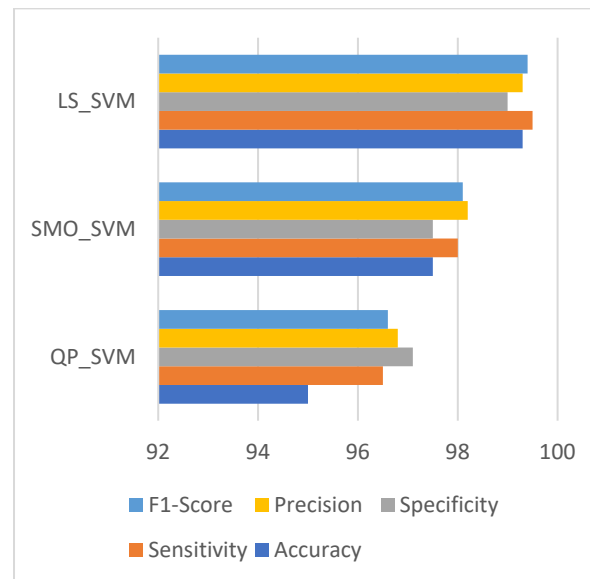


**Figure 11.** Performance of Different SVM types for Hybrid features.

Finally, we compared our proposed algorithms with other recent works in the literature that used the same Bern-Barcelona database, as shown in Table 7. From the table, the proposed algorithms in this work showed improvements in performance as compared with some recent work that experimented with the same dataset. Bhattacharyya et al. [12] used reconstructed phase space (RPS), EWT, and LS\_SVM to characterize focal and non-focal EEG signals and obtained an accuracy of 90%. Acharya et al. [51] employed nonlinear features and reported an accuracy of 87.93%. Details of comparison can be found in Figure 7 and Section 5.3.

**Table 7.** Comparison of recent works that used the same database with our work and our proposed method.

Author	Year	Feature Extraction	Type of Classifier	Accuracy(%)
Bhattacharyya et al. [53]	2017	Fuzzy Entropy, FAWT	LS-SVM	84.67
Sharma et al. [54]	2017	Entropies, WFB	LS-SVM	94.25
Gupta et al. [46]	2017	Entropy, FAWT	LS-SVM	94.40
Sharma et al. [55]	2018	Time-domain, IMFs	LS-SVM	84.01
Bhattacharyya et al. [15]	2018	RPS, EWT	LS-SVM	90.0
Acharya et al. [56]	2018	Nonlinear Features	LS-SVM	87.93
Zhao et al. [57]	2018	Entropies	CNN	83.0
Arunkumar, et al. [18]	2018	Entropies	Exemplars classifier	99.0
Gupta and Pachori [58]	2019	Entropies, IMFs	LS-SVM	83.18
Subasi et al. [59]	2019	WPT	Random Forest	99.2
Daoud and Bayoumi [60]	2020	DCAE	MLP	93.2
Fraïwan and Alkhodari [24]	2020	B-LSTM	B-LSTM	99.60
Sue et al. [61]	2021	STFT	CNN	94.3
This study	2022	DWT, hybrid	1D-CNN	99.4
This study	2022	Hybrid Features	LS_SVM	99.3
This Study	2022	WT-SST	2D-DCNN	99.7

### 5.3. Performance of the Models Based on Execution Time

The execution time was computed to further evaluate the performance of the proposed method; the time was calculated at different stages, which included the time required for preprocessing, EEG signal decomposition, feature extraction, k-fold training, and testing of the model. Figure 12 shows the execution time of our various proposed methods. From the Figure, the combined features with DNN (Hybrid-DNN) require longer to classify the focal and non-focal EEG signals with an execution time of 13.2 s, while the WSST-



DCNN only took around 11.3 s. These values indicate that the proposed methods could be used in real-time and online applications. Moreover, by using higher computationally optimized software, the time required to execute the algorithm could be further decreased. A comparison of our proposed model's execution time with other work provided in Table 7 is not shown, as none of the work provided the time required to implement their proposed method.

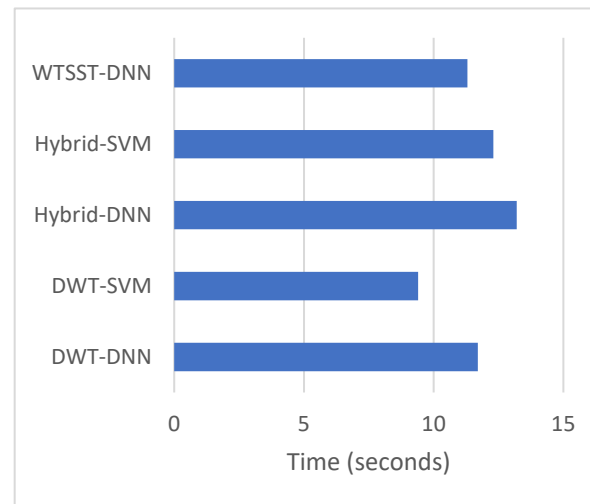


**Figure 12.** Execution time of the proposed models.

## 6. Discussion

The detection and location of epileptogenic zones in epilepsy patients is a vital step for drug-resistant cases requiring surgery. We proposed various methods that help classify focal and non-focal EEG signals in order to develop an efficient CAD system by extracting relevant and significant features that are suitable for use in portable devices such as IoMT devices. These features are then passed on to various proposed classifiers, such as SVM, KNN, Random Forest, 1D-CNN, and 2D-DCNN. We also explored the advantages of an improved version of the synchrosqueezing transform called WT-SST that provides a tight energy distribution in the time-frequency domain features when compared to conventional DWT. This property of WT-SST is capable of characterizing the pathological signs of focal and non-focal EEG signals. Several researchers have exploited the efficacy of various features from different domains such as the time-domain, frequency-domain, time-frequency-domain, nonlinear entropy, and statistical features.

Our proposed approach was evaluated using the accuracy, sensitivity, specificity, precision, and F1-score as performance parameters. From the results presented in Section 4. The time-domain raw EEG signals were decomposed using the DWT domain; the extracted features were classified using the LS-SVM and 1D-CNN networks. The performance of the method using 1D-CNN was 98.8%, 97.3%, 97.7%, 98.8%, and 98.0% for accuracy, sensitivity, specificity, precision, and F1-score, respectively. Combined hybrid features from different domains were experimented on with SVM and 2D-DCNN, and the proposed techniques showed improved performance when compared to the DWT-CNN technique. The highest score was obtained using the proposed WTSST-DCNN structure with an accuracy, sensitivity, specificity, precision, and F1-score of 99.7%, 99.5%, 99.7%, 99.7%, and 99.6%, respectively.

We used average accuracy to compare the performance results of our proposed techniques with other related works that employed the same Bern-Barcelona database in their study, as tabulated in Table 5. The authors in [53] classified focal and non-focal EEG signals using the features extracted from multivariate EEG signals using TQWT. Multivariate fuzzy entropy was computed and extracted from these sub-bands features, LS-SVM was deployed in the classification stage, and the performance accuracy was recorded as 84.67%.

The authors in [54] utilized the benefit of wavelet transform for the classification of focal and non-focal EEG signals; they proposed a feature extraction technique by calculating entropies from the orthogonal wavelet filter banks coefficients that are localized in time-frequency. They obtained an accuracy of 94.25% after classifying the EEG signals with an LS-SVM classifier. Entropy features such as approximate entropy, fuzzy entropy, and sample entropy were computed in [18] as features for focal and non-focal EEG signal classification. They experimented with the features using various classifiers, and the best accuracy of 99.0% was achieved with the Non-Nested Generalized Exemplars classifier. Recently, authors in [58] computed IMFs from the EMD technique, and the entropy features were calculated from IMFs as features for the LS-SVM classifier; a classification accuracy of 83.18% was successfully achieved. Another work that used the same database is that of Subasi et al. [59]. In their study, the performance of features from different domains such as EMD, WPD, and DWT with multi-scale PCA and random forest classifier was conducted, and an accuracy of 99.2% was achieved with a reduced version of the dataset. Recently, some authors explored the deep learning application in the detection and classification of focal and non-focal EEG signals, as reported in [60]. A deep convolutional autoencoder was proposed with a k-means clustering algorithm, and an accuracy of 93.2% was recorded. Other recent work includes Sue et al. [61], who used hybrid network structures of conventional feature extraction techniques such as STFT analysis combined with 1D and 2D convolutional neural networks. An accuracy of 94.3% was reported as the best performance accuracy obtained from the hybrid deep CNN model.

One of the important aspects of improving the accuracy of epileptic seizure detection systems is the preprocessing stage. In this work, we employed a bandpass filter for the elimination and removal of the artifacts embedded in the epileptic EEG signals. However, other advanced preprocessing methods could be deployed in future work to improve the performance of the model aimed at the development of low-cost EEG monitoring and BCI systems. Recently, work presented in [62,63] has demonstrated an efficient and advanced method for the elimination of eye blink artifacts using variational mode extraction (VME) with DWT and clustering algorithm approaches based on variational mode extraction (VME) and smoothed nonlinear energy operator (SNEO), respectively. Another factor to be considered for improving the efficiency of our method is to investigate the optimal values of the nonlinear features by tuning the appropriate parameters to obtain an optimal value. This work employed a *t*-test statistical method to optimize the parameters based on their lowest *p*-value. Other parameter optimization methods should be considered in future work to properly tune some parameters to their optimal values.

Few previous works have reported on the application of localization for epileptogenic areas in the brain EEG signals using a deep learning approach, as it is mostly applied in areas of image processing. This work aims to leverage the application of deep learning networks in the analysis of EEG epileptic seizure signals. The work includes a comprehensive analysis of various feature extraction techniques proposed by various researchers; these features are either from the EEG signals themselves or from the sub-bands of the signals. The performance of conventional classifiers, such as SVM, was compared with that of recent deep neural networks, such as the CNN architecture. We tried to explore how the hand-crafted features could be combined with DNN architectures as well as how these DNN architectures could be used as a stand-alone classifier without the need for hand-crafted features. We have also seen how the learnable feature maps in our proposed DCNN network properly discriminate and characterize the information hidden in the EEG signals to detect and classify focal and non-focal EEG signals.

## 7. Conclusions

This work aims to develop an automated computer-aided scheme for the efficient location of epileptogenic zones through the classification of focal and non-focal EEG signals. The study developed three (3) different and novel algorithms with competitively high accuracy relative to recent works (see Table 7). Among these proposed schemes, WT-SST with a 2D-DCNN

network (WTSST-DCNN) had the highest accuracy of 99.7%, with 10-fold cross-validation in the classification process. This was owing to its tight energy in the time-frequency domain. The time-frequency, statistical, and nonlinear analyses were combined to form a hybrid technique with an accuracy of 99.4%, while the DWT-hybrid had an accuracy of 99.3%. These algorithms are less computationally complex, hence their potential application in IoMT devices. In future work, various DNN structures, such as deep transformer models, should be considered, and the hybridization within these networks should be explored and experimented on. In addition, other datasets from the public domain and non-public datasets should be considered.

**Author Contributions:** Conceptualization, S.S., G.X. and I.A.K.; methodology, S.S. and I.A.E.K.; software, S.S. and I.A.E.K.; validation, S.S., G.X. and Z.S.; formal analysis, S.S. and Y.K.A.; data curation, S.S. and I.S.A.; writing—original draft preparation, S.S. and Y.K.A.; writing—review and editing, S.S., Y.K.A. and A.H.J.; supervision, G.X. and Z.S.; project administration, G.X. and Z.S.; funding acquisition, G.X. All authors have read and agreed to the published version of the manuscript.

**Funding:** This work was supported in part by the National Natural Science Foundation of China under Grant (51737003 and Grant 51977060); this work was also supported by the Specialized Research Fund for the Doctoral Program of Higher Education under Grant (20121317110002) and Grant (20131317120007).

**Data Availability Statement:** The data used in this paper is available at the following website: [https://www.upf.edu/web/ntsa/downloads/-/asset\\_publisher/xvT6E4pczrBw/content/2012-nonrandomness-nonlinear-dependence-and-nonstationarity-of-electroencephalographic-recordings-from-epilepsy-patients#.Yk2zpZTMK1s](https://www.upf.edu/web/ntsa/downloads/-/asset_publisher/xvT6E4pczrBw/content/2012-nonrandomness-nonlinear-dependence-and-nonstationarity-of-electroencephalographic-recordings-from-epilepsy-patients#.Yk2zpZTMK1s) (accessed on 5 October 2019).

**Conflicts of Interest:** The authors declare no conflict of interest.

## Abbreviations

ANN	artificial neural network
ApEn	approximate entropy
AR	autoregressive
CAD	computer-aided diagnosis
CNN	convolutional neural network
DBF	deep belief network
DCNN	deep convoluted neural network
DNN	deep neural network
DWT	discrete wavelet transform
EEG	electroencephalogram
EESC	epileptic EEG signal classification
EOG	electrooculogram
EWT	empirical wavelet transform
FAWT	flexible analytic wavelet transform
GPU	graphics processing unit
GRU	gated recurrent unit
HOS	higher-order spectra
ICA	independent component analysis
IMF	intrinsic mode function
IoMT	internet of medical things
KNN	k-nearest neighbor
LMSLS-SVM	least mean square/least square support vector machine
LSTMB-LSTM	long short-term memory/Bidirectional-LSTM
MCA	morphological component analysis
MRI	magnetic resonance imaging
NB	naive Bayes
NLMS	non-local means
PCA	principal component analysis
PSD	power spectral density
PNN	probabilistic neural network

RLS	recursive least square
RPS	reconstructed phase space
STFT	short time Fourier transform
SVM	support vector machine
SMO-SVM	sequential minimal optimization-SVM
SSDA	stacked sparse density autoencoders
TCNN	temporal CNN
TQWT	tunable Q-wavelet decomposition
QP-SVM	Quadratic Programming-SVM
WPE	wavelet packet entropy
WT	wavelet transform
WT-SST	wavelet transform-synchrosqueezing transform

## References

- World Health Organization. Available online: <http://www.who.int/newsroom/fact-sheets/detail/epilepsy> (accessed on 17 February 2020).
- Fisher, R.S.; Acevedo, C.; Arzimanoglou, A.; Bogacz, A.; Cross, J.H.; Elger, C.E.; Engel, J., Jr.; Forsgren, L.; French, J.A.; Glynn, M. ILAE official report: A practical clinical definition of epilepsy. *Epilepsia* **2014**, *55*, 475–482. [CrossRef] [PubMed]
- Falco-Walter, J.J.; Scheffer, I.E.; Fisher, R.S. The new definition and classification of seizures and epilepsy. *Epilepsy Res.* **2018**, *139*, 73–79. [CrossRef] [PubMed]
- Siuly, S.; Zhang, Y. Medical big data: Neurological diseases diagnosis through medical data analysis. *Data Sci. Eng.* **2016**, *1*, 54–64. [CrossRef]
- Yuen, A.W.; Keezer, M.R.; Sander, J.W. Epilepsy is a neurological and a systemic disorder. *Epilepsy Behav.* **2018**, *78*, 57–61. [CrossRef]
- Siuly, S.; Li, Y.; Zhang, Y. *EEG Signal Analysis and Classification: Techniques and Applications*; Springer: Berlin/Heidelberg, Germany, 2017.
- Shahbakhti, M.; Beiramvand, M.; Eigirdas, T.; Solé-Casals, J.; Wierchcon, M.; Broniec-Wójcik, A.; Augustyniak, P.; Marozas, V. Discrimination of Wakefulness from Sleep Stage I Using Nonlinear Features of a Single Frontal EEG Channel. *IEEE Sens. J.* **2022**, *22*, 6975–6984. [CrossRef]
- Shahbakhti, M.; Beiramvand, M.; Rejer, I.; Augustyniak, P.; Broniec-Wójcik, A.; Wierchcon, M.; Marozas, V. Simultaneous Eye Blink Characterization and Elimination from Low-Channel Prefrontal EEG Signals Enhances Driver Drowsiness Detection. *IEEE J. Biomed. Health Inform.* **2022**, *26*, 1001–1012. [CrossRef]
- Lin, S.; Istiqomah; Wang, L.; Lin, C.; Chiueh, H. An Ultra-Low Power Smart Headband for Real-Time Epileptic Seizure Detection. *Wearable Sens. Health Monit. Syst.* **2018**, *6*, 2700410. [CrossRef]
- Gavvala, J.; Abend, N.; LaRoche, S.; Hahn, C.; Herman, S.T.; Claassen, J.; Macken, M.; Schuele, S.; Gerard, E.; Critical Care EEG Monitoring Research Consortium (CCEMRC). Continuous EEG monitoring: A survey of neurophysiologists and neurointensivists. *Epilepsia* **2014**, *55*, 1864–1871. [CrossRef]
- Saminu, S.; Xu, G.; Zhang, S.; Isselmou, A.K.; Jabire, A.H.; Ahmed, Y.K.; Karaye, I.A.; Ahmad, I.S. A Recent Investigation on Detection and Classification of Epileptic Seizure Techniques Using EEG Signal. *Brain Sci.* **2021**, *11*, 668. [CrossRef]
- Hu, L.; Zhang, Z. *EEG Signal Processing and Feature Extraction*; Springer Nature: Singapore, 2019.
- Saminu, S.; Xu, G.; Zhang, S.; Isselmou, A.E.K.; Jabire, A.H.; Karaye, I.A.; Ahmad, I.S. Hybrid feature extraction technique for multi-classification of ictal and non-ictal EEG epilepsy signals. *Elektr. J. Electr. Eng.* **2020**, *19*, 1–11. [CrossRef]
- Saminu, S.; Xu, G.; Zhang, S.; Isselmou, A.E.K.; Zakariyya, R.S.; Jabire, A.H. Epilepsy detection and classification for smart IoT devices using hybrid technique. In Proceedings of the 15th International Conference on Electronics, Computer and Computation (ICECCO), Abuja, Nigeria, 10–12 December 2019; pp. 1–6.
- Bhattacharyya, A.; Sharma, M.; Pachori, R.B.; Sircar, P.; Acharya, U.R. A novel approach for automated detection of focal EEG signals using empirical wavelet transform. *Neural Comput. Appl.* **2018**, *29*, 47–57. [CrossRef]
- Raghu, S.; Srimaam, N. Classification of focal and non-focal EEG signals using neighborhood component analysis and machine learning algorithms. *Expert Syst. Appl.* **2018**, *113*, 18–32. [CrossRef]
- Kumar, M.R.; Rao, Y.S. Epileptic seizures classification in EEG signal based on semantic features and variational mode decomposition. *Clust. Comput.* **2019**, *22*, 13521–13531. [CrossRef]
- Arunkumar, N.; Kumar, K.R.; Venkataraman, V. Entropy features for focal EEG and non-focal EEG. *J. Comput. Sci.* **2018**, *27*, 440–444. [CrossRef]
- Dalal, M.; Tanveer, M.; Pachori, R.B. Automated Identification system for Focal EEG Signals Using Fractal Dimension of FAWT-Based Sub-bands Signals. In *Machine Intelligence and Signal Analysis*; Springer: Singapore, 2019; Volume 748, pp. 583–596.
- Deivasigamani, S.; Senthilpari, C.; Wong, H.Y. Computer Aided Automatic Detection and Classification of EEG Signals for Screening Epilepsy Disorder. *J. Inf. Sci. Eng.* **2018**, *34*, 687–700.

21. Gao, Z.; Lu, G.; Yan, P.; Lyu, C.; Li, X.; Shang, W. Automatic Change Detection for Real-Time Monitoring of EEG Signals. *Front. Physiol.* **2018**, *9*, 325. [[CrossRef](#)]
22. Srirangan, M.; Tripathy, R.K.; Pachori, R.B. Time-frequency domain deep convolutional neural network and non-focal EEG signals. *IEEE Sens.* **2020**, *20*, 3078–3086.
23. Poomipat, B.; Apiwat, L.; Jitkomut, S. Automatic epileptic seizure onset-offset detection based on CNN in scalp EEG. In Proceedings of the 2020 IEEE International Conference on Acoustics, Speech and Signal Processing (ICASSP), Barcelona, Spain, 4–8 May 2020; pp. 1225–1229.
24. Fraiwan, L.; Alkhodari, M. Classification of non-focal and focal Epileptic patients using single channel EEG and Long short-term memory learning system. *IEEE Access* **2020**, *8*, 77255–77262. [[CrossRef](#)]
25. Raheel, A.; Sajid, S.; Syed, A.H.; Soltan, A.; Awais, M.K. Epileptic seizure detection with a reduced montage: A way forward for Ambulatory EEG devices. *IEEE Access* **2020**, *8*, 65880–65890.
26. Wei, Z.; Mengqing, L.; Chenzhi, Y.; Qinghui, W.; Fenglin, L.; Ying, W. Classification of focal and non-focal EEG signals using empirical mode decomposition (EMD), phase space reconstruction and neural networks. *Artif. Intell. Rev.* **2019**, *52*, 625–647.
27. Yang, Y.; Wanzhong, C.; Mingyang, L.; Tao, J.; Yun, J.; Xiao, Z. Automatic focal and non-focal EEG detection using entropy based features from flexible analytic wavelet transform. *Biomed. Signal Process. Control* **2020**, *57*, 101761.
28. Md Mosheyur, R.; Mohammed, I.H.B.; Anindya, B.D. Classification of focal and non-focal EEG signals in VMD-DWT domain using ensemble stacking. *Biomed. Signal Process. Control* **2019**, *50*, 72–82.
29. Jose, A.; Mario, R.A.; Alejandro, Z.; Tripathy, R.K.; Pachori, R.B. EEG-Rhythm specific Taylor-Fourier bank implemented with O-splines for the detection of epilepsy using EEG signals. *IEEE Sens.* **2020**, *20*, 6542–6551.
30. Raghu, S.; Pradip, S.; Pachori, R.B. Automated focal EEG signal detection based on third order cumulant function. *Biomed. Signal Process. Control* **2020**, *58*, 101856.
31. Saminu, S.; Özkurt, N.; Karaye, I.A. Wavelet Feature Extraction for ECG Beat Classification, An Appraisal. In Proceedings of the 6th International Conference on Adaptive Science and Technology (ICAST 2014), Ota, Nigeria, 29–31 October 2014; pp. 350–355.
32. Faust, O.; Acharya, U.R.; Adeli, H.; Adeli, A. Wavelet-based EEG processing for computer-aided seizure detection and epilepsy diagnosis. *Seizure Eur. J. Epilepsy* **2015**, *26*, 56–64. [[CrossRef](#)] [[PubMed](#)]
33. Kaushik, G.; Sinha, D.H. Biomedical Signal Analysis through Wavelets: A Review. *Int. J. Adv. Res. Comput. Sci. Softw. Eng.* **2012**, *2*, 422–428.
34. Saminu, S.; Özkurt, N. Stationary wavelet transform and entropy-based features for ECG beat classification. *Int. J. Res. Stud. Sci. Eng. Technol.* **2015**, *2*, 23–32.
35. Yu, G.; Wang, Z.; Zhao, P. Multisynchrosqueezing transform. *IEEE Trans. Ind. Electron.* **2018**, *66*, 5441–5455. [[CrossRef](#)]
36. Daubechies, I.; Lu, J.; Wu, H.T. Synchrosqueezed wavelet transforms: An empirical mode decomposition-like tool. *Appl. Comput. Harmon. Anal.* **2011**, *30*, 243–261. [[CrossRef](#)]
37. Wang, S.; Chen, X.; Tong, C.; Zhao, Z. Matching synchrosqueezing wavelet transform and application to aeroengine vibration monitoring. *IEEE Trans. Instrum. Meas.* **2016**, *66*, 360–372. [[CrossRef](#)]
38. Panachake, J.T.; Ramakrishnan, A.G.; Ananthapadmanabha, T.V. Decoding Imagined Speech using Wavelet Features and Deep Neural Networks. In Proceedings of the 2019 IEEE 16th India Council International Conference (INDICON), Rajkot, India, 13–15 December 2019.
39. Isselmou, A.E.K.; Xu, G.; Shuai, Z.; Saminu, S.; Javaid, I.; Ahmad, I.S.; Kamhi, S. Brain Tumor Detection and Classification on MR Images by a Deep Wavelet Auto-Encoder Model. *Diagnostics* **2021**, *11*, 1589.
40. Faust, O.; Hagiwara, Y.; Hong, T.J.; Lih, O.S.; Acharya, U.R. Deep learning for healthcare applications based on physiological signals: A review. *Comput. Methods Programs Biomed.* **2018**, *161*, 1–13. [[CrossRef](#)] [[PubMed](#)]
41. Cudlenco, N.; Popescu, N.; Leordeanu, M. Reading into the mind's eye: Boosting automatic visual recognition with EEG signals. *Neurocomputing* **2020**, *386*, 281–292. [[CrossRef](#)]
42. LeCun, Y.; Bengio, Y.; Hinton, G. Deep learning. *Nature* **2015**, *521*, 436–444. [[CrossRef](#)]
43. Sargül, M.; Ozyildirim, B.; Avci, M. Differential convolutional neural network. *Neural Netw.* **2019**, *116*, 279–287. [[CrossRef](#)]
44. Isselmou, A.E.K.; Xu, G.; Shuai, Z.; Saminu, S.; Javaid, I.; Ahmad, I.S. Differential Deep Convolutional Neural Network Model for Brain Tumor Classification. *Brain Sci.* **2021**, *11*, 352.
45. Das, A.B.; Bhuiyan, M.I.H. Discrimination and classification of focal and non-focal EEG signals using entropy-based features in the EMD-DWT domain. *Biomed. Signal Process. Control* **2016**, *19*, 11–21. [[CrossRef](#)]
46. Gupta, V.; Priya, T.; Yadav, A.K.; Pachori, R.B.; Acharya, U.R. Automated detection of focal EEG signals using features extracted from flexible analytic wavelet transform. *Pattern Recognit. Lett.* **2017**, *94*, 180–188. [[CrossRef](#)]
47. Tripathy, R.K.; Bhattacharyya, A.; Pachori, R.B. Localization of myocardial infarction from multi-lead ECG signals using multiscale analysis and convolutional neural network. *IEEE Sens. J.* **2019**, *19*, 11437–11448. [[CrossRef](#)]
48. Chen, B.; Wang, X.; Lu, N.; Wang, S.; Cao, J.; Qin, J. Mixture correntropy for robust learning. *Pattern Recognit.* **2018**, *79*, 318–327. [[CrossRef](#)]
49. Andrzejak, R.G.; Schindler, K.; Rummel, C. Nonrandomness, nonlinear dependence and non-stationarity of electroencephalographic recordings from epilepsy patients. *Phys. Rev. E* **2012**, *86*, 046206. [[CrossRef](#)] [[PubMed](#)]
50. Siddharth, T.; Pranjali Gajbihiye, P.; Tripathy, R.K.; Ram Bilas Pachori, R.M. EEG based Detection of Focal Seizure Area using FBSE-EWT rhythm and SAE-SVM Network. *IEEE Sens. J.* **2020**, *20*, 11421–11428. [[CrossRef](#)]



51. Sharmila, A. Epilepsy detection from EEG signals: A review. *J. Med. Eng. Technol.* **2018**, *42*, 368–380. [[CrossRef](#)] [[PubMed](#)]
52. Akbari, H.; Sadiq, M.T. Detection of focal and non-focal EEG signals using non-linear features derived from empirical wavelet transform rhythms. *Phys. Eng. Sci. Med.* **2021**, *44*, 157–171. [[CrossRef](#)]
53. Bhattacharyya, A.; Pachori, R.; Acharya, U. Tunable-q wavelet transform based multivariate sub-band fuzzy entropy with application to focal eeg signal analysis. *Entropy* **2017**, *19*, 99. [[CrossRef](#)]
54. Sharma, M.; Dhere, A.; Pachori, R.B.; Acharya, U.R. An automatic detection of focal EEG signals using new class of time-frequency localized orthogonal wavelet filter banks. *Knowl. Based Syst.* **2017**, *118*, 217–227. [[CrossRef](#)]
55. Sharma, R.R.; Varshney, P.; Pachori, R.B.; Vishvakarma, S.K. Automated system for epileptic EEG detection using iterative filtering. *IEEE Sens. Lett.* **2018**, *2*, 1–4. [[CrossRef](#)]
56. Acharya, U.R.; Hagiwara, Y.; Deshpande, S.N.; Suren, S.; Koh, J.E.W.; Oh, S.L.; Arunkumar, N.; Ciaccio, E.J.; Lim, C.M. Characterization of focal eeg signals: A review. *Future Gener. Comput. Syst.* **2018**, *91*, 290–299. [[CrossRef](#)]
57. Zhao, X.; Zhao, Q.; Tanaka, T.; Cao, J.; Kong, W.; Sugano, H.; Yoshida, N. Detection of epileptic foci based on interictal iEEG by using convolutional neural network. In Proceedings of the 2018 IEEE 23rd International Conference on Digital Signal Processing (DSP), Shanghai, China, 19–21 November 2018; pp. 1–5.
58. Gupta, V.; Pachori, R.B. A new method for classification of focal and non-focal EEG signals. In *Machine Intelligence and Signal Analysis*; Springer: Berlin/Heidelberg, Germany, 2019; pp. 235–246.
59. Subasi, A.; Jukic, S.; Kevric, J. Comparison of emd, dwt and wpd for the localization of epileptogenic foci using random forest classifier. *Measurement* **2019**, *146*, 846–855. [[CrossRef](#)]
60. Daoud, H.; Bayoumi, M. Deep learning approach for epileptic focus localization. *IEEE Trans. Biomed. Circuits Syst.* **2020**, *14*, 209–220. [[CrossRef](#)]
61. Sui, L.; Zhao, X.; Zhao, Q.; Tanaka, T.; Cao, J. Hybrid Convolutional Neural Network for Localization of Epileptic Focus Based on iEEG. *Neural Plast.* **2021**, *2021*, 6644365. [[CrossRef](#)] [[PubMed](#)]
62. Shahbakhti, M.; Beiramvand, M.; Nazari, M.; Broniec-Wójcik, A.; Augustyniak, P.; Rodrigues, A.S.; Wierzchon, M.; Marozas, V. VME-DWT: An Efficient Algorithm for Detection and Elimination of Eye Blink From Short Segments of Single EEG Channel. *IEEE Trans. Neural Syst. Rehabil. Eng.* **2021**, *29*, 408–417. [[CrossRef](#)] [[PubMed](#)]
63. Wang, M.; Wang, J.; Cui, X.; Wang, T.; Jiang, T.; Gao, F.; Cao, J. Multidimensional Feature Optimization Based Eye Blink Detection Under Epileptiform Discharges. *IEEE Trans. Neural Syst. Rehabil. Eng.* **2022**, *30*, 905–914. [[CrossRef](#)] [[PubMed](#)]